Experimental investigation of the electronic structure of $Gd_5Ge_2Si_2$ by photoemission and x-ray absorption spectroscopy

2007 J. Phys.: Condens. Matter 19 186219

(http://iopscience.iop.org/0953-8984/19/18/186219)

IOP PUBLISHING JOURNAL OF PHYSICS: CONDENSED MATTER

J. Phys.: Condens. Matter **19** (2007) 186219 (14pp) doi:10.1088/0953-8984/19/18/186219

Experimental investigation of the electronic structure of $Gd_5Ge_2Si_2$ by photoemission and x-ray absorption spectroscopy

F Bondino[1], A Brinkman[2,3], M Zangrando[1], F Carbone[2], D van der Marel[2], D L Schlagel[4], T A Lograsso[4], K A Gschneidner Jr[4,5], V K Pecharsky[4,5] and F Parmigiani[1,6,7,8]

[1] Laboratorio Nazionale TASC INFM-CNR, Basovizza-Trieste, Italy
[2] Département de Physique de la Matière Condensée, Université de Genève, CH-1211 Genève, Switzerland
[3] Faculty of Science and Techology and MESA + Institute for Nanotechnology, University of Twente, The Netherlands
[4] Materials and Engineering Physics Program, Ames Laboratory, Iowa State University, Ames, IA 50011-3020, USA
[5] Department of Materials Science and Engineering, Iowa State University, Ames, IA, 50011-2300, USA
[6] Dipartimento di Fisica, Università degli Studi di Trieste, Trieste, Italy
[7] Dipartimento di Matematica e Fisica, Università Cattolica del Sacro Cuore, Brescia, Italy
[8] Sincrotrone Trieste S.C.p.A., Basovizza-Trieste, Italy

E-mail: bondino@tasc.infm.it

Received 27 November 2006, in final form 1 March 2007
Published 11 April 2007
Online at stacks.iop.org/JPhysCM/19/186219

Abstract

The electronic structure of the magnetic refrigerant $Gd_5Ge_2Si_2$ has been experimentally investigated by photoemission and x-ray absorption spectroscopy. The resonant photoemission and x-ray absorption measurements performed across the Gd $N_{4,5}$ and Gd $M_{4,5}$ edges identify the position of Gd 4f multiplet lines, and assess the 4f occupancy ($4f^7$) and the character of the states close to the Fermi edge. The presence of Gd 5d states in the valence band suggests that an indirect 5d exchange mechanism underlies the magnetic interactions between Gd 4f moments in $Gd_5Ge_2Si_2$. From 175 to 300 K the first 4 eV of the valence band and the Gd partial density of states do not display clear variations. A significant change is instead detected in the photoemission spectra at higher binding energy, around 5.5 eV, likely associated to the variation of the bonding and antibonding Ge(Si) s bands across the phase transition.

1. Introduction

$Gd_5Ge_2Si_2$ is a strongly correlated electron system with entangled structural and magnetic properties that are of great interest to fundamental studies and potential applications [1]. The

ternary compound undergoes a magnetic transition from a low-temperature ferromagnetic to a high-temperature paramagnetic phase at a Curie temperature (T_C) that nearly linearly increases from 276 to 330 K as the magnetic field rises from, respectively, 0 to 10 T [2–4]. The magnetic phase transition is accompanied by a first-order structural phase transformation from orthorhombic symmetry (space group $Pnma$, no. 62) below T_C to monoclinic symmetry (space group $P112_1/a$, no. 14) above T_C [5].

The observation of a magnetic field dependent T_C [2], a giant magnetocaloric effect between 270 and 300 K [2–4, 6], a colossal magnetostriction [7, 8], and a large negative magnetoresistance [9] around the phase transition boundary, together with magnetic field dependent x-ray powder diffraction [10, 11] and differential scanning calorimetric [12, 13] studies of $Gd_5Ge_2Si_2$ and related compounds indicate that externally applied magnetic fields can alter both the magnetic and crystal structures of $Gd_5Ge_2Si_2$. The same is true for numerous other members of the extended family of $Gd_5(Ge_{4-x}Si_x)$ materials. The magneto-responsiveness of these compounds makes them potentially useful for applications as active components of magnetostrictive transducers, magnetoresistive sensors, magnetomechanical devices, and magnetic refrigerators.

Although the structural, electrical, thermal, and magnetic properties of the $Gd_5Ge_2Si_2$ phase have been rather well investigated experimentally [2, 3, 5, 14–30], the electronic structure of this system is almost unknown, with the exception of the valence band (VB) measured by x-ray and ultraviolet photoelectron spectroscopy (PES) [31].

Electronic band structure calculations do exist in the literature [32–37], but the calculations rely heavily on a set of assumptions derived from available experimental data of elemental Gd, which the authors urge are in need of experimental verification, e.g. for the strong-coupling Coulomb correlation parameter U between 4f electrons.

Furthermore, the microscopic mechanism of the ferromagnetism in $Gd_5Ge_2Si_2$ has not been clarified yet. The Ruderman–Kittel–Kasuya–Yosida (RKKY) indirect exchange [38] has been suggested as a possible mechanism [5, 39], since the interslab Si/Ge–Si/Ge bonding in this distinctly layered material changes across the phase transition, giving rise to a change in valence electron concentration and unit-cell volume. The idea is, that the structural phase transition from the high-temperature monoclinic phase to the low-temperature ferromagnetic orthorhombic phase is characterized by a shortening of the interslab Si/Ge–Si/Ge distances, while all intraslab Gd–Gd distances basically remain unchanged [39]. The electronic structure consequently changes from having antibonding to covalent bonding Si/Ge–Si/Ge states, and the spectral weight at the Fermi level increases due to the combined enhanced valence and decreased unit-cell volume [36]. However, increasing the Fermi momentum would shift the first zero-crossing of the RKKY function to smaller distances, reducing the exchange coupling at constant Gd–Gd distance [38][9]. The only way for the RKKY function to be relevant is to consider its second zero-crossing. The exchange integral in this case is, however, much smaller.

Alternatively, Morellon *et al* [8] suggest that a change in density of states at the Fermi level can modify the sign of the conduction-band indirect exchange interaction due to a competition between first- and second-order superexchange perturbation [40]. For rare earth metals in general, a different indirect exchange has been proposed by Campbell [41], in which the rare earth creates a positive local d moment through the ordinary f–d exchange.

Direct d–d interactions, as in transition metals, then determine the sign of the coupling between f electron spins (see [41]). Band-structure calculations [31] and spectroscopic measurements of the valence band [31, 42] of several $Gd_5(Ge_{4-x}Si_x)$ compounds with $x = 0, 2,$

[9] The spin-polarization of a conduction band electron (approximated as a free electron) is antiparallel to the magnetic impurity in the RKKY model for small distances, then parallel for larger distances, etc. The resulting exchange coupling in RKKY is favouring parallel spin alignment of two impurities (or in our case f spins) for small distances.

and 4 support the idea that Gd 5d electrons are relevant to the magnetism of the system. It is, therefore, interesting to investigate in detail the electronic structure of $Gd_5Ge_2Si_2$; in particular, it is important to assess the character of the itinerant electrons in the VB and identify the Gd partial density of states (DOS) in the VB.

In this work, we report the electronic structure of $Gd_5Ge_2Si_2$ investigated by means of PES and x-ray absorption spectroscopy (XAS). The photon energy dependence of valence band photoemission and the elemental selectivity of resonant photoemission (resPES) across Gd absorption edges have been exploited to single out the contribution of the Gd partial DOS close to the Fermi energy E_F and detect possible variations across T_C.

2. Experimental methods

The experiments were performed at the BACH beamline of Elettra in Trieste [43, 44]. Polarized light in the 35–1600 eV range is provided by two APPLE II helical undulators. For the XAS measurements, the monochromator resolution was set to 1 eV in the Gd $M_{4,5}$ photon energy range and 0.08 eV in the Gd $N_{4,5}$ energy range.

Single crystals of $Gd_5Ge_2Si_2$ were produced from appropriate quantities of pure gadolinium (99.996 wt% Gd), silicon (99.9999 wt% Si), and germanium (99.999 wt% Ge) that were arc melted several times under an argon atmosphere[10]. The arc-melted polycrystalline material was then used as the charge material in a tri-arc crystal-pulling furnace [45]. A tungsten rod was used as the seed material, which resulted in a randomly oriented $Gd_5Ge_2Si_2$ crystal. The as-grown crystal was oriented by the back-reflection Laue technique and the crystallographic directions were verified using x-ray diffraction θ–2θ scans of the single crystal.

The photoemission measurements were performed using a 150 mm VSW hemispherical electron analyser with a 16-channel detector. The absorption spectra were recorded in total electron yield, collecting simultaneously the drain current from the sample and a reference drain current I_0 from the last refocusing mirror as a function of the incident photon energy. The XAS data were normalized by the reference I_0. The resolution of the photoemission spectra is determined as the convolution of the energy resolution of the photon beam and the energy resolution of the VSW analyser. The value is calculated as a function of the slit opening, photon energy and pass energy from semi-empirical formulae that have been obtained and experimentally verified in previous characterizations of the beamline and the electron analyser.

The sample, mounted with the *b*-axis perpendicular to the surface, was fractured periodically. The pressure in the chamber was always lower than 5×10^{-10} mbar. From the freshly fractured sample we have obtained all the surface-sensitive valence band photoemission spectra across the $N_{4,5}$ edge and $N_{4,5}$ edge XAS measurements at different temperatures. The spectra at higher photon energy ($h\nu > 500$ eV) were acquired after the sample was sputtered using 500 eV Ar ions after verifying the nominal 5:2:2 stoichiometry and the absence of O 1s and C 1s core-level peaks in the sample. The Gd/Ge stoichiometry was estimated from a direct comparison of the spectra obtained from the sputtered sample and the fractured sample acquired in the same experimental conditions at 1168 eV photon energy. The normalized spectra were identical within the noise level (<4%). Measurements at lower energy (∼560 eV) also showed that the areas of Gd 4f, Si 2p and Ge 3d core levels were the same as for the sputtered and the fractured sample. However, in this case, the fractured sample showed a little of contamination, so the correct stoichiometry of the sputtered surface was confirmed from the cross-section weighted intensity of Gd 4f, Si 2p and Ge 3d photoemission core levels, considering the

[10] Gadolinium was prepared by the Materials Preparation Center, Ames Laboratory US-DOE, Ames, USA, www.mpc.ameslab.gov; silicon and germanium were purchased from Meldform Metals, Inc.

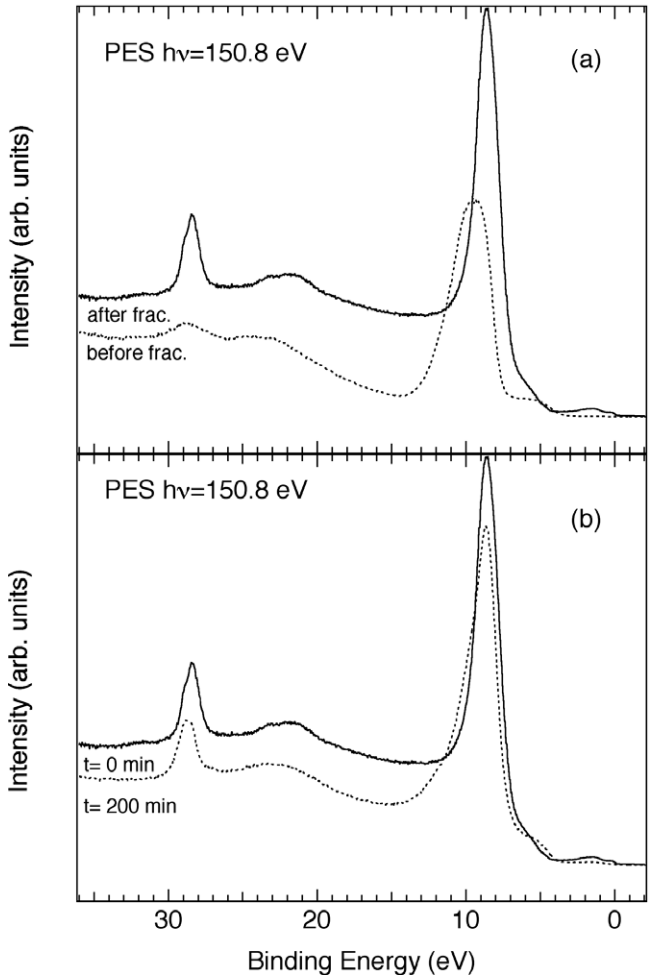

Figure 1. (a) VB normalized PES spectra obtained at $h\nu = 150.8$ eV before and after fracturing the sample surface at 300 K. (b) VB spectra measured at $h\nu = 150.8$ eV just after fracturing the sample and after 200 min in a base pressure of 4×10^{-10} mbar.

analyser transmission and the inelastic mean free path variation with kinetic energy from the NIST data base [46] using the Tanuma, Powell and Penn formula [47].

Surface cleanliness was checked continuously by monitoring the O 1s and the Si 2p core levels and the VB.

Figure 1(a) shows the changes observed in a VB PES spectrum obtained at $h\nu = 150.8$ eV before and after fracturing the sample surface at 300 K. The measurements obtained before fracturing are obtained from a sample exposed to the atmosphere for several weeks. The two spectra have been normalized to the photon flux and the spectra have been acquired with a total energy resolution of 0.093 eV. After the fracture, spectral weight appears at binding energies (BEs) between E_F and 2 eV, the structure around 5 eV is suppressed, the doublet around 21.7–23 eV from the Gd $5p_{3/2}$ core level can be resolved, the intensity of Ge 3d peak around 28–29 eV BE increases, and the Ge 3d line shape shifts and changes. A shift of ∼0.9 eV to lower BE is also observed in the Gd 4f multiplet lines of $Gd_5Ge_2Si_2$, which are centred at ∼8.5 eV

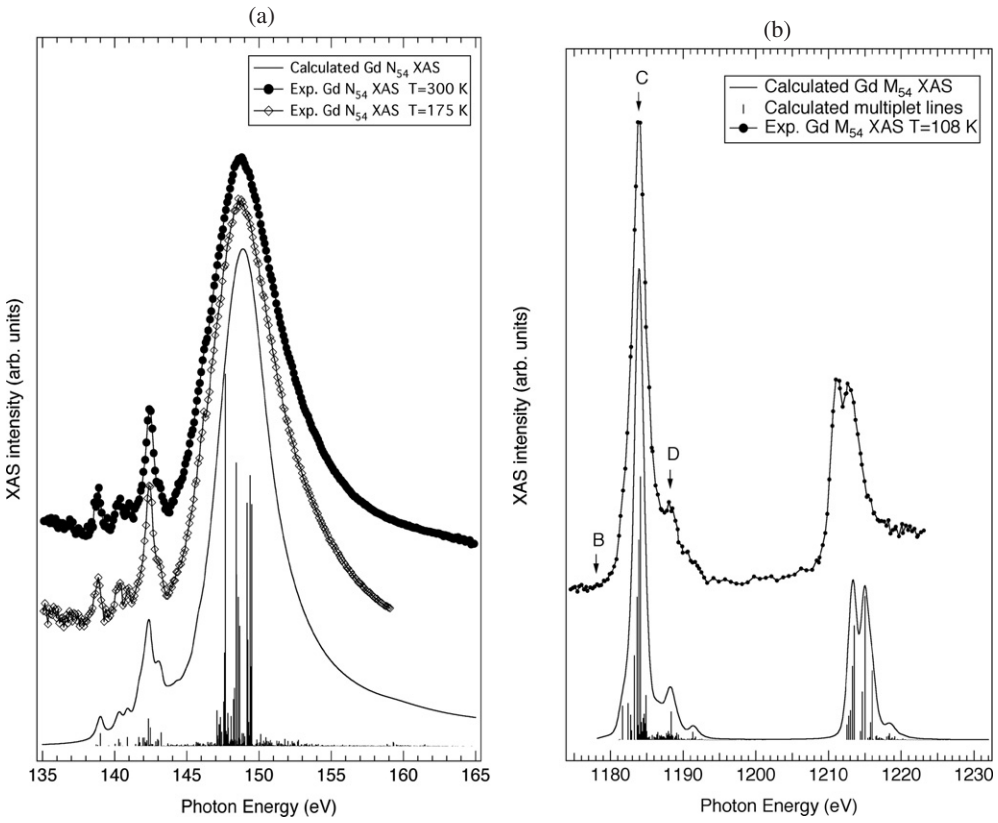

Figure 2. (a) The Gd $N_{4,5}$ XAS spectra measured at 300 and 175 K compared with the result of a multiplet calculation performed for a $[Xe]4f^7$ configuration. (b) The Gd $M_{4,5}$ XAS spectrum measured at 108 K is compared with the result of a multiplet calculation performed for a $[Xe]4f^7$ configuration. Three of the photon energies, corresponding to the resPES spectra of figure 4, are indicated and labelled B, C and D in the depicted spectrum.

BE after the fracture. Furthermore (not shown here), after the fracture, the BE of Si 2p core level shifts from ∼102.3 to ∼98–99 eV.

The effect of surface degradation on VB spectra measured at $h\nu = 150.8$ eV in a base pressure of 4×10^{-10} mbar is shown in figure 1(b). The two spectra have been normalized to the photon flux. We observed a relatively fast degradation of the crystal surface, as seen from the depletion of the states close to E_F, the growing of a component with BE around 5–6 eV, the growing of new components at the high-BE side of the Gd 4f peaks, and a gradual intensity decrease and shift to higher BEs of the Ge 3d core level.

3. Results and discussion

The Gd $N_{4,5}$ XAS spectra, measured at 300 K (above T_C) and 175 K (below T_C) immediately after fracturing the sample surface, are displayed in figure 2(a), while in figure 2(b), the Gd $M_{4,5}$ XAS spectrum (uncalibrated energy scale) measured at 108 K is shown. Above T_C, an identical Gd $M_{4,5}$ XAS lineshape is measured (not shown here). The experimental Gd $N_{4,5}$ and Gd $M_{4,5}$ XAS spectra are well reproduced by XAS multiplet atomic calculations with the

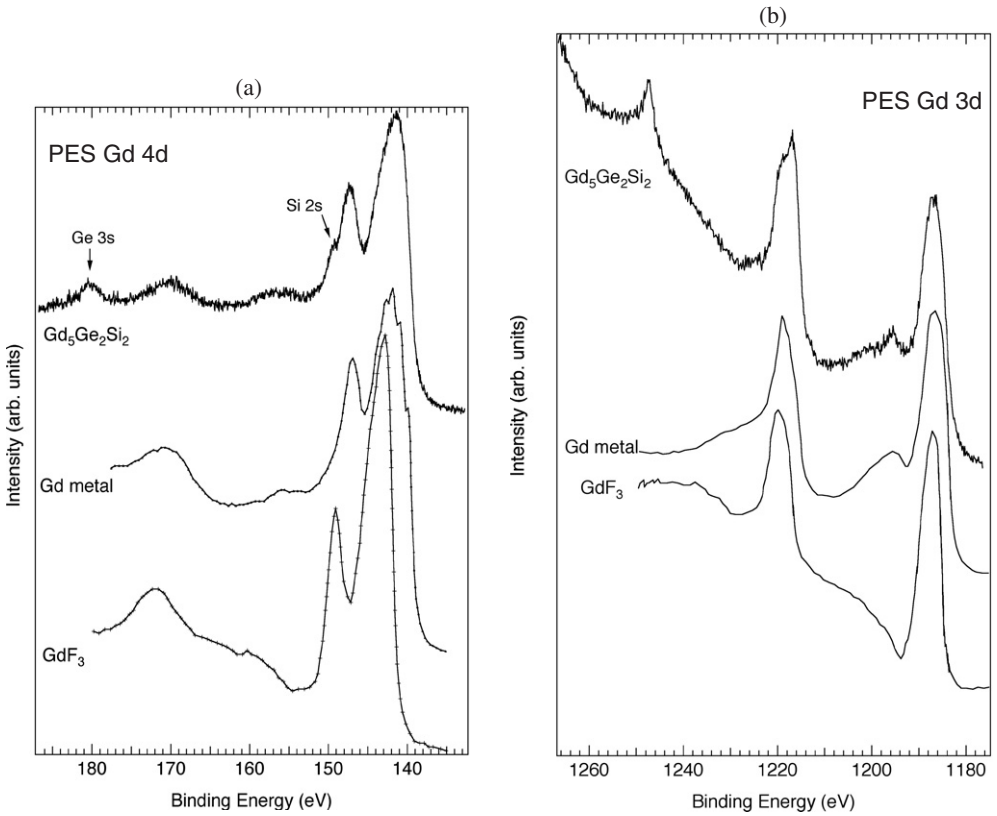

Figure 3. (a) The Gd 4d core level obtained from $Gd_5Ge_2Si_2$ at 300 K with $h\nu = 566.7$ and a total energy resolution of 0.29 eV, together with the corresponding spectra of metallic Gd and GdF_3, as extracted from [48]. Peaks corresponding to Ge 3s (∼180.5 eV) and Si 2s (∼150 eV) emissions in $Gd_5Ge_2Si_2$ are indicated by arrows. (b) The Gd 3d (∼1187 and ∼1220 eV) and Ge 2p (∼1217 and ∼1248 eV) core levels obtained from $Gd_5Ge_2Si_2$ at 300 K with $h\nu = 1379.1$ eV, together with the corresponding spectra of metallic Gd and GdF_3, as extracted from [48].

$4f^7$ configuration in spherical symmetry. No variation across the transition is observed in the $GdM_{4,5}$ and $N_{4,5}$ XAS line shapes of $Gd_5Ge_2Si_2$, indicating that the Gd 4f occupancy remains unchanged.

The presence of Gd itinerant electrons has been investigated by PES, studying both the contribution of Gd states in the VB and the Gd core levels.

The Gd 4d core level spectrum, obtained at 300 K with $h\nu = 566.7$ eV and a total energy resolution of 0.29 eV, is shown in figure 3(a). In the spectrum, a structure is present around a BE = 150 eV due to Si 2s emission, as well as a peak due to Ge 3s around BE = 180.5 eV. The experimental spectrum is displayed together with the Gd 4d spectra of Gd metal and GdF_3, as extracted from [48]. The Gd 4d spectra exhibit a complex line distribution, determined by the intra-atomic interaction between the 4d core hole and the 4f shell. The Gd 4d spectrum is separated by the exchange interaction in a low-BE region resonance between 140 and 150 eV with several narrow peaks (unresolved in the spectrum of $Gd_5Ge_2Si_2$) and a higher-BE region above 150 eV with broad lines.

The Gd 4d core-level multiplet manifold of $Gd_5Ge_2Si_2$ displays a large energy shift (∼2–3 eV) to lower BE with respect to that of GdF_3 (figure 3(a)), while they are at the same

BE positions as the Gd metal 4d core level from Szade *et al* [48]. In spite of the comparable energy resolution of these measurements (0.29 eV) and those of Szade *et al* (0.35 eV) [48, 49], the linewidth of the low-BE multiplets (between ∼145 and 150 eV) in $Gd_5Ge_2Si_2$ is larger than for Gd metal and the multiplets cannot be resolved as separate peaks in the spectrum. This observation can be related to a shorter lifetime of these states, similarly to what happens for Gd_5Si_4. The differences with respect to the ionic compounds can be related to the presence of conduction electrons, while the larger width of the low-BE multiplets with respect to the Gd metal is likely being due to the fact that a fraction of the valence electrons is involved in covalent bonding with Si atoms [48]. A relation between the intensity of the satellite at 155–160 eV and the density of sp electrons at the Fermi level has been suggested [49]. The intensity of this satellite in $Gd_5Ge_2Si_2$ is high, compared to the measurements of Szade *et al* on several intermetallic compounds (with exception of $GdIn_3$), but is comparable to the intensity in Gd metal [49]. Thus both the lineshape and the BE position the Gd 4d core level indicate the presence in the VB of Gd itinerant electrons, in part involved in covalent bonding.

Figure 3(b) shows the Gd 3d (∼1187 and ∼1220 eV) and Ge 2p core levels (∼1217 and ∼1248 eV) obtained from $Gd_5Ge_2Si_2$ at 300 K with $h\nu = 1379.1$ eV and a total energy resolution of 0.84 eV. The spectrum of $Gd_5Ge_2Si_2$ is compared to the Gd 3d PES spectra from ionic GdF_3 and Gd metal, as extracted from [48]. Between BE 1217 and 1220 eV, Ge $2p_{3/2}$ overlaps with the Gd $3d_{3/2}$ core level.

The Gd 3d PES spectrum in $Gd_5Si_2Ge_2$ (figure 3(b)) exhibits strong and broad satellites on the high-BE side of the main Gd 3d peaks (between 1194 and 1208 eV). A strong intensity of these satellites is also found in Gd metal, while they are much weaker in GdF_3 (figure 3(b)). Since the strength of these satellites is influenced by the presence of Gd VB electrons [48], the lineshape of Gd 3d is also consistent with the presence of a finite density of Gd itinerant states in the VB.

Figure 4 shows a set of VB spectra measured at 108 K across the GdM_5 absorption edge at the photon energies B, C and D (1178, 1184 and 1188 eV), as labelled in the XAS spectrum of figure 2(b), and additionally at A ($h\nu = 1162.1$ eV). The spectra have been normalized to the photon flux and acquired with a total resolution of 0.73 eV. As the photon energy is varied across the edge, a structure located at about 8.5 eV BE, associated with Gd $4f^7$ F_J multiplets [50], is strongly enhanced. At the photon energy corresponding to the absorption satellite D in the XAS spectrum, a structure at ∼5 eV higher BE with respect to the main ^7F_J multiplets is observed. This component resonates at the photon energy corresponding to satellite D of the absorption spectrum of figure 2(b) and, from our data, appears at constant binding energy. A similar component at a constant binding energy was already observed in Gd metal and assigned to the ^5X multiplet structure [51].

The difference spectrum, obtained by subtracting the off-resonance spectrum A from one of the on-resonance spectra C, is shown in the bottom panel of figure 4. In the difference spectrum, besides the pronounced structure attributed to Gd $4f^7F_J$ multiplets, a structure centred around 1.5–2 eV is present (see inset), which is related to the Gd partial DOS. The same results are obtained at 300 K (above T_C) in GdM_5 resPES measurements (not shown here).

The broad component centred at about 24 eV, extending from 20 to 30 eV, is a superposition of Gd 5p (3/2 and 1/2) and Ge 3d. In particular, Gd $5p_{3/2}$ multiplets are located around 21–23.5 eV (see figure 1). Gd $5p_{1/2}$ emission should be located around 27–28 eV according to measurements on Gd metal and other Gd metallic compounds [52], but this component is probably hidden by the Ge 3d emission at about 28.5 eV. Even if this is not clear from the available data, an Auger emission may also be superimposed on the core levels, determining the broad shape.

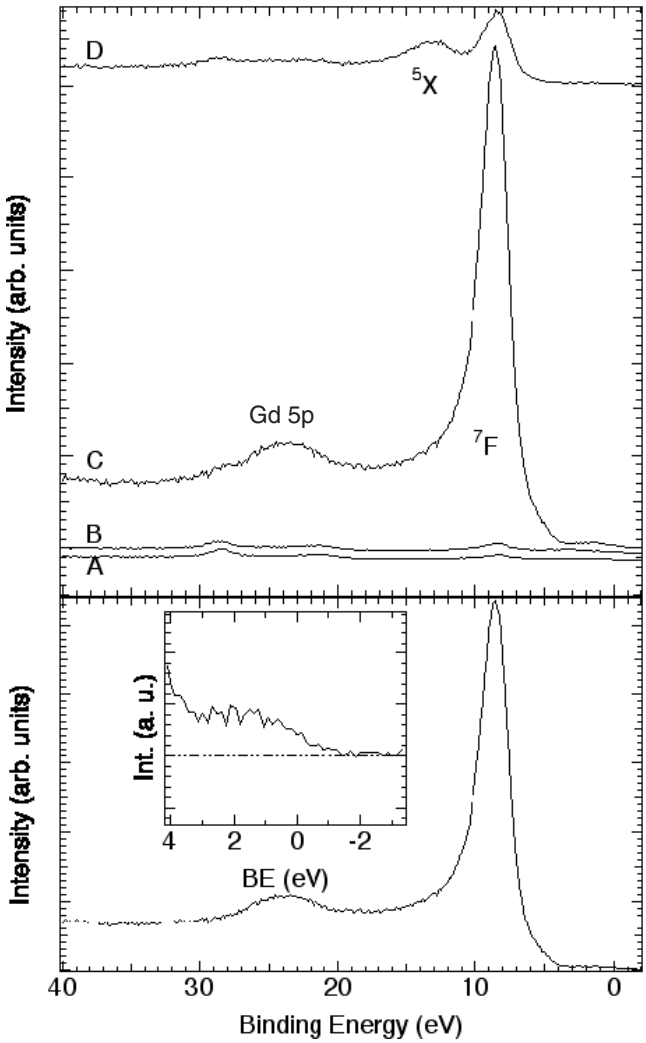

Figure 4. Top panel: a set of normalized VB resPES spectra measured at 108 K across the GdM_5 absorption edge at the photon energies B ($h\nu = 1178$ eV), C ($h\nu = 1184$ eV, on resonance) and D ($h\nu = 1188$ eV), as labelled in figure 2(b), and at the energy A ($h\nu = 1162.1$ eV, off resonance). Bottom panel: the difference between the spectra measured at energies C and A.

Figure 5(a) shows the VB spectra at 175 K (below T_C) normalized to the photon flux, measured with a photon energy on the Gd $N_{4,5}$ absorption maximum at 149.3 eV and off-resonance at 135.6 eV (total resolution ∼0.14 eV). The photon energies correspond to the triangles in the inset of figure 5(a). The difference spectrum between the on-resonance and off-resonance Gd $N_{4,5}$ spectra is shown in figure 5(b). In this difference spectrum, the Gd ^7F_J 4f multiplet lines extend over a narrow BE range (less than 1 eV) centred at ∼8.5 eV.

A shoulder around 6 eV appearing in the Gd $N_{4,5}$ resPES spectrum (figure 5) does not appear to be related to the $4f^7$ multiplets from the comparison with the theoretical predictions. Considering local spin density approximation (LSDA) + U calculations for $Gd_5Ge_2Si_2$ [32], this structure can be associated to Si 3s and Ge 4s states hybridized with Gd sp states, since they are expected to be located at 2–3 eV lower BE than the Gd 4f levels.

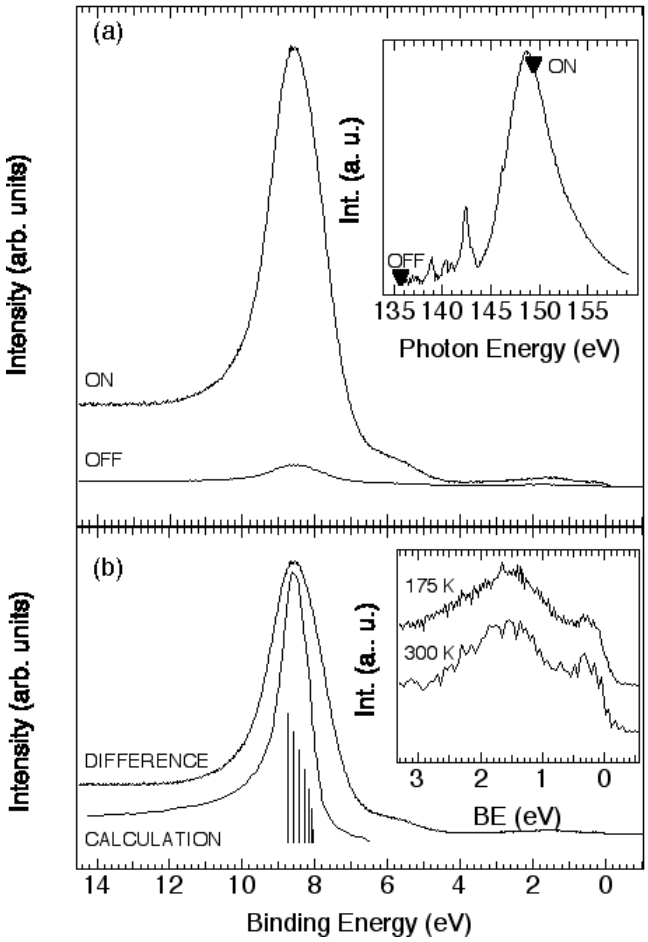

Figure 5. (a) VB spectra normalized to the photon flux and measured across the Gd $N_{4,5}$ absorption edge, on resonance at 149.3 eV, and off resonance at 135.6 eV at 175 K, below T_C. The photon energies correspond to the triangles (ON and OFF) in the inset of (a). (b) The difference between the spectra measured on and off resonance compared to a Gd 4f PES calculation reproduced from [55]. In the inset, a close-up of the difference spectrum on the BE region close to E_F measured at 175 K is shown and compared to the same difference spectrum obtained at 300 K.

The difference spectrum in the energy region from E_F to 3.3 eV is reported in the inset of figure 5(b) and compared to the difference spectrum obtained at 300 K. No significant differences are observed between the two spectra. Both above and below T_C a narrow peak around 0.3 eV followed by a dip around 0.5 eV and a broad structure with BE centred around 1.55 eV are observed, with an identical ratio (of both the area and the intensity) between the 1.55 eV and 0.3 peaks. These structures showing an enhancement at the Gd $N_{4,5}$ absorption maximum are associated with Gd states and do not appear to change significantly between 175 and 300 K.

A temperature variation in the photoemission spectra is observed instead in the energy region from 4.5 to 6.5 eV. This variation is barely visible in the on–off difference spectra, while it appears significant in the photoemission spectra acquired at 135.6 eV, shown in figure 6. While the first 4 eV of the spectra are identical, the structure around 5.5 eV appears narrower

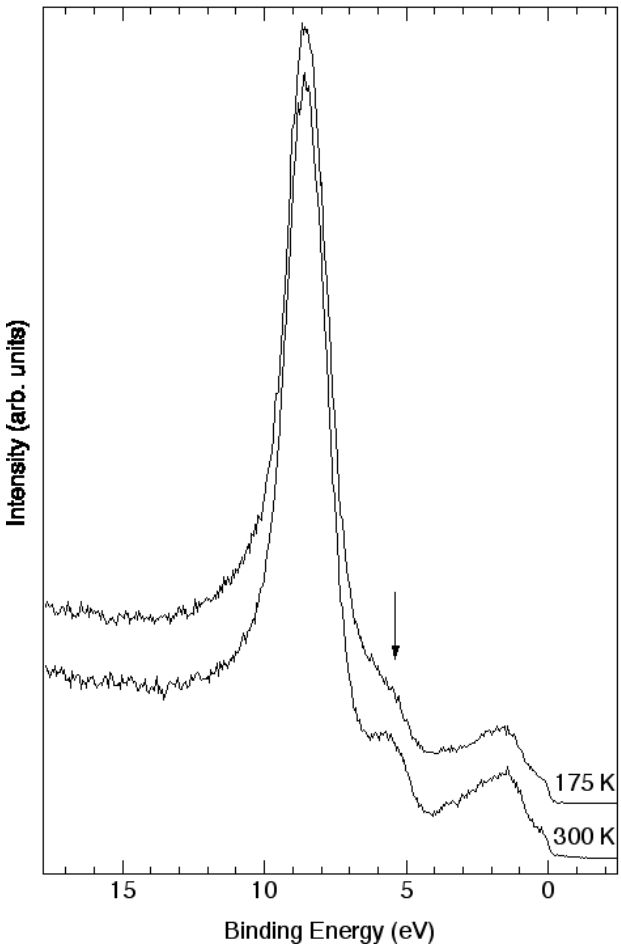

Figure 6. Comparison of the photoemission spectra measured at 135.6 eV at 175 K and at 300 K, in both cases just after the sample fracture. The spectra are normalized to the Gd 4f peak. The arrow indicates the structure at 5.5 eV that displays the temperature variation.

and slightly more pronounced above T_C. We observe that the energy position of this structure also corresponds to a contamination component (see figure 1). However, both the 175 and 300 K spectra have been acquired in the same conditions only a few (2–3) minutes after the sample fracture in good vacuum conditions, and the other structures (the VB states close to E_F, Gd 4f and Si 2p core levels) are identical above and below T_C with no signals of contamination (broadening, energy shifts, growing of germanium or silicon oxides). So this effect can be associated to an actual variation of the electronic structure. This electronic-structure variation is likely connected to the structural changes occurring across the phase transition at 270 K in which the interslab (Si, Ge)–(Si, Ge) dimers that are richer in Ge increase their distances (bond 'breaking'). Indeed, calculations indicate that these elongated bonds should give rise to a decrease of the splitting and a common upward shift of the bonding and antibonding Ge(Si) s bands [53]. According to the calculations [32], Si 3s and Ge 4s states should be located on the low-BE side of the Gd 4f levels and are less hybridized with Gd states than Ge(Si) p bands. Thus, the observed narrowing of the structure around 5.5 eV, located just at the bottom side

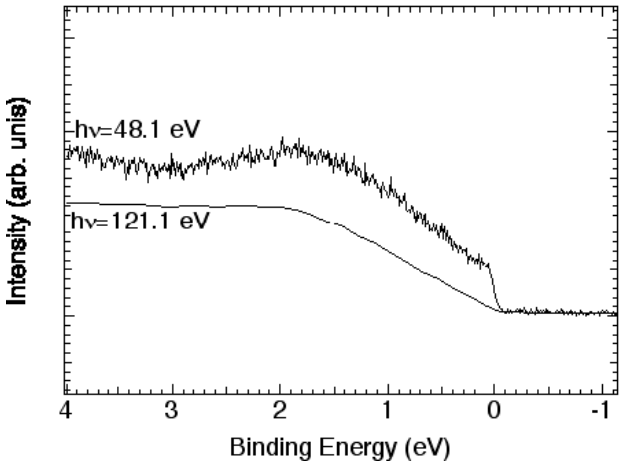

Figure 7. VB spectra measured at 48.1 and 121.1 eV at 108 K normalized to the photon flux.

of the Gd 4f level, can be likely associated to the predicted change of the Ge(Si) s bonding–antibonding bands due to the bond elongation across T_C.

A comparison of the $Gd_5Ge_2Si_2$ VB measured at two different photon energies (48.1 and 121.1 eV) is shown in figure 7. The VB obtained at $h\nu = 121.1$ eV (total resolution ∼0.148 eV) does not show clear peaks, but, between 4.0 and 1.8 eV, a nearly constant spectral weight which then slopes down to E_F. The VB obtained at $h\nu = 48.1$ eV (total resolution ∼0.022 eV) exhibits a broad structure with BE around 1.8 eV and a clear Fermi edge. At $h\nu = 48.1$ eV, the cross section of the structure around 1.8 eV is strongly enhanced with respect to the spectrum at $h\nu = 121.1$ eV, where Gd 5d has its Cooper minimum and where the Si 3sp and Ge 4sp cross sections dominate. The two structures close to E_F at BE = 1.55 eV and 0.3 eV observed in the difference between the on-resonance and off-resonance $GdN_{4,5}$ spectra (figure 5(b)) do not appear in the VB of $Gd_5Ge_2Si_2$ acquired with $h\nu = 121.1$ eV, on the Gd Cooper minimum. This further confirms their Gd origin (figure 5). The structure at ∼0.3 eV can be assigned to Gd 5d states in analogy with Gd metal. DOS calculations for Gd_5Si_4 and Gd_5Ge_4 also found predominant Gd 5d character in this energy region close to E_F [31]. The same calculations [31] indicate that the broad structure at 1.55 eV can be attributed to Gd 5d 6p–Si 3p hybridized states.

The Gd 4f multiplet lines of $Gd_5Ge_2Si_2$, which are centred at ∼8.5 eV (figures 1 and 5), are shifted by ∼1.9 eV towards lower BE with respect to GdF_3 and Gd_2O_3 [48, 54], while they are at about the same BE as in metallic Gd [54], with a tendency of the Gd 4f level to be located at higher BE in ionic compounds. A shift towards lower BE is also observed in Gd 4f after the fracture from the clean sample surface with respect to the contaminated surface where some GdO_x was likely present (figure 1(a)). The 4f multiplet position at 8.5 eV can be used to obtain the important U_{eff} input parameter in LSDA + U first-principles calculations. A U_{eff} of 6.7 eV provides a total splitting between the 4f levels above and below the Fermi energy of 11 eV and a BE of 8.5 eV [32], consistent with our experimental observation.

The $4f^7$ configuration for Gd, derived from the $M_{4,5}$ and $N_{4,5}$ XAS measurements, is consistent with the results of bulk magnetic measurements that found an effective magnetic moment of 7.89 μ_B for $Gd_5Ge_2Si_2$ single crystals, corresponding to a $4f^7(Gd^{3+})$ configuration [42]. No change was observed in the 4f occupancy across the phase transition.

Based on the photoemission experiments discussed in the previous section, we have arrived at the conclusion that, in $Gd_5Si_2Ge_2$, the bands at the Fermi energy are of primarily Gd 5d and

Ge 4sp (Si 3sp) character. The phase transition is known to have occurred at 260 K when cooling down and 270 K when warming up, from bulk magnetic susceptibility measurements on the same sample.

Across T_C, photoemission spectra detect a variation in the energy window between 4.5 and 6.5 eV from E_F, related to a predicted change in the energy in energy distribution of Ge(Si) s states and associated to the elongation of the Ge(Si)–Ge(Si) interatomic distance.

The question arises what it means that no clear changes are observed in the 0–4 eV energy range at the two sides of the phase transition.

A possible destruction of the phase transition at the surface is not likely to happen. The depth probed by the present Gd $N_{4,5}$ resPES measurements is only approximately 10 Å, and surface effects cannot be ruled out. However, in previous XPS measurements [31] performed at 1486 eV, where the probed sample depth was about five times deeper, variations in the valence band from 233 to 303 K could not be observed in the same binding energy range.

A more likely explanation of the lack of change in the 0–4 eV energy region of the spectra is the subtlety of the changes in electronic structure combined with the sensitivity of the photoemission spectra.

Calculations [36, 39] indicate that changes in the electronic states through the phase transition should affect the energy distribution of Ge/Si sp states. In particular, it is predicted that the phase transition leads to a change of the Fermi level and a change of the conduction bandwidth. The presence of elongated Si/Ge bonds in the high-temperature phase should give rise, besides to an upward shift and a decrease of the splitting of the bonding and antibonding s bands [53], also to a reduced splitting of bonding and antibonding p bands, causing new spectral features around 0.65 and 1.1 eV for the majority spin, and around 0.5 and 0.1 eV for the minority spin in the partial density of states [37]. However, other calculations point out the difficulty of noticing major changes in the electronic states close to E_F through the phase transition due to the strong Gd 5d–Si/Ge p hybridization, although the variations are expected to appear more clearly in the energy distribution of Ge 4s states at higher binding energies [32]. The optical spectra, for instance, are predicted to be only slightly changed in the 0–1 eV energy range [32]. Thus, the lack of variations in the first 4 eV from E_F in the present measurements is likely due to the very strong Gd 5d–Si/Ge p hybridization. Other spectroscopic measurements are more suitable for observing electronic changes across the phase transition. Angle-resolved photoemission measurements would allow a disentanglement of the band and its dispersion around the 0.65 eV structure. Magneto-optical spectroscopy is also predicted to be more sensitive to the phase transition than conventional optical measurements. Transport measurements are suitable for an accurate determination of the total density of states. For example, the strong anisotropy observed in the magnetoresistance [37] has suggested that there is a significant reduction of electronic velocity in the [100] direction across the phase transition related to a large contribution to the DOS at the Fermi level from Si atoms.

The clear narrow structure that appears close to E_F at 0.3 eV is attributed to Gd–Gd bonding or the remaining 5d band. The 5d character of the bands plays an important role in the ferromagnetic coupling, because, as has been argued by Campbell, 'the direct d–d interaction should continue to dominate for rare earth compounds with nontransition elements as long as rare earth concentrations are sufficient for d–d overlaps to remain possible. This condition is crystal structure dependent but on the whole means rare earth concentrations greater than 50%' [41]. Indeed, this condition is satisfied in $Gd_5Si_2Ge_2$, in accordance with the observed ferromagnetism. The fact that also at temperatures above the phase transition spectral weight with 5d character is present does not weaken the relevance of the 5d states to the magnetic mechanism below the phase transition.

4. Conclusion

PES, resPES and XAS measurements have been performed on $Gd_5Ge_2Si_2$ single crystal in order to investigate the electronic properties of this compound across the phase transition at 276 K. The measurements indicate that all Gd ions have occupancy of 7 electrons in the 4f shell both above and below the magneto-structural phase transition, consistent with the conclusions of previous magnetic measurements. The BE position and the lineshapes of Gd core levels (3d, 4d, 4f) show a strong similarity with Gd metallic compounds and clear differences with respect to ionic Gd compounds. Since the Gd core levels are strongly influenced by solid-state effects, and since they appear related to the Gd VB states close to E_F, these measurements already suggest the presence of itinerant Gd electrons in the VB and covalent bonding of a fraction of these electrons with Si and Ge atoms.

This is confirmed by resPES, that also offers a better characterization of the VB states. The Gd partial DOS in the VB is localized precisely and directly in the difference spectra obtained by subtracting the off-resonance spectra from the on-resonance PES spectra with the photon energy tuned on Gd $N_{4,5}$ and Gd M_5 XAS maxima. Both above and below T_C, the difference spectra show a clear spectral weight associated with Gd states between E_F and the Gd 4f multiplets with a narrow feature at 0.3 eV and a broad structure around 1.55 eV. The Gd 5d itinerant electrons are expected to be responsible for the magnetic exchange interaction between the Gd 4f local moments.

No clear changes are observed in the 0–4 eV binding energy region, for temperatures above and below the magneto-structural transition, meaning that potentially subtle changes in Gd 5d and Si(Ge) p states across the phase transition remain to be investigated by other means. Variations are instead observed in the off-resonance spectra in the energy window between 4.5 and 6.5 eV. These variations can be associated to the predicted changes in the energy distribution of Ge(Si) s states due to the presence of elongated Ge(Si) bonds in the high-temperature phase.

Acknowledgments

Work at Ames Laboratory is supported by the Office of Basic Energy Sciences, Materials Sciences Division of the US Department of Energy, under contract No. W-7405-ENG-82 with Iowa State University. Work at beamline BACH was supported by FIRB project No. RBNE0155X7.

References

[1] Pecharsky V K and Gschneidner K A Jr 2001 *Adv. Mater.* **13** 683
[2] Pecharsky V K and Gschneidner K A Jr 1997 *Phys. Rev. Lett.* **78** 4494
[3] Pecharsky V K and Gschneidner K A Jr 1997 *J. Magn. Magn. Mater.* **167** L179
[4] Pecharsky V K and Gschneidner K A Jr 1997 *Appl. Phys. Lett.* **70** 3299
[5] Choe W, Pecharsky V K, Pecharsky A O, Gschneidner K A Jr, Young V G Jr and Miller G J 2000 *Phys. Rev. Lett.* **84** 4617
[6] Pecharsky V K and Gschneidner K A Jr 1998 *Adv. Cryog. Eng.* **43** 1729
[7] Morellon L, Algarabel P A, Ibarra M R, Blasco J, García-Landa B, Arnold Z and Albertini F 1998 *Phys. Rev.* B **58** R14721
[8] Morellon L, Blasco J, Algarabel P A and Ibarra M R 2000 *Phys. Rev.* B **62** 1022
[9] Morellon L, Stankiewicz J, García-Landa B, Algarabel P A and Ibarra M R 1998 *Appl. Phys. Lett.* **73** 3462
[10] Pecharsky V K, Holm A P, Gschneidner K A Jr and Rink R 2003 *Phys. Rev. Lett.* **91** 197204
[11] Pecharsky V K and Gschneidner K A Jr 2005 *Magnetism and Structure in Functional Materials* (*Springer Series in Materials Science* vol 79) ed A Planes, L Mañosa and A Saxena (Heidelberg: Springer) chapter 11, p 199

[12] Casanova F, Batlle X, Labarta A, Marcos J, Mañosa L and Planes A 2002 *Phys. Rev.* B **66** 212402
[13] Casanova F, Batlle X, Labarta A, Marcos J, Mañosa L and Planes A 2003 *J. Appl. Phys.* **93** 8313
[14] Giguère A, Foldeaki M, Ravi Gopal B, Chahine R, Bose T K, Frydman A and Barclay J A 1999 *Phys. Rev. Lett.* **83** 2262
[15] Levin E M, Pecharsky V K and Gschneidner K A Jr 1999 *Phys. Rev.* B **60** 7993
[16] Pecharsky V K and Gschneidner K A Jr 1999 *J. Appl. Phys.* **86** 6315
[17] Gschneidner K A Jr, Pecharsky V K, Brück E, Duijn H G M and Levin E M 2000 *Phys. Rev. Lett.* **85** 4190
[18] Sun J R, Hu F X and Shen B G 2000 *Phys. Rev. Lett.* **85** 4191
[19] Levin E M, Pecharsky V K and Gschneidner K A Jr 2000 *Phys. Rev.* B **62** R14625
[20] Meyers J, Chumbley S, Choe W and Miller G J 2002 *Phys. Rev.* B **66** 012106
[21] Pecharsky A O, Gschneidner K A Jr and Pecharsky V K 2003 *J. Appl. Phys.* **93** 4722
[22] Lee S J, Park J M, Snyder J E, Jiles D C, Schlagel D L, Lograsso T A, Pecharsky A O and Lynch D W 2004 *Appl. Phys. Lett.* **84** 1865
[23] Nersessian N, Or S W, Carman G P, Choe W, Radousky H B, McElfresh W, Pecharsky V K and Pecharsky A O 2004 *Appl. Phys. Lett.* **84** 4801
[24] Vecchini C, Moze O, Pecharsky A O, Pecharsky V K, Gschneidner K A Jr, Brück E, Bewley R and Klesnikov A 2004 *J. Appl. Phys.* **95** 7207
[25] Provenzano V, Shapiro A J and Shull R D 2004 *Nature* **429** 854
[26] Mudryk Y, Lee Y, Vogt T, Gschneidner K A and Pecharsky V K Jr 2005 *Phys. Rev.* B **71** 174104
[27] Magen C, Morellon L, Algarabel P A, Ibarra M R, Arnold Z, Kamarad J, Lograsso T A, Schlagel D L, Pecharsky V K, Tsokal A O and Gschneidner K A Jr 2005 *Phys. Rev.* B **72** 024416
[28] Carvalho A M G, Alves C S, de Campos A, Coelho A A, Gama S, Gandra F C G, von Ranke P J and de Oliveira N A 2005 *J. Appl. Phys.* **97** 10M320
[29] Mozharivskyj Y, Pecharsky A O, Pecharsky V K and Miller G J 2005 *J. Am. Chem. Soc.* **127** 317
[30] Ugurlu O, Chumbley L S, Schlagel D L and Lograsso T A 2005 *Acta Mater.* **53** 3525
[31] Skorek G, Deniszczyk J and Szade J 2002 *J. Phys.: Condens. Matter* **14** 7273
[32] Harmon B N and Antonov V N 2002 *J. Appl. Phys.* **91** 9815
[33] Harmon B N and Antonov V N 2003 *J. Appl. Phys.* **93** 4678
[34] Harmon B N, Antonov V N, Lichtenstein A I, Solovyev I V and Anisimov V I 1995 *J. Phys. Chem. Solids* **56** 1521
[35] Rhee J Y 2003 *J. Korean Phys. Soc.* **43** 621
[36] Samolyuk G D and Antropov V P 2005 *J. Appl. Phys.* **97** 10A310
[37] Tang H, Pecharsky V K, Samolyuk G D, Zou M, Gschneidner K A Jr, Antropov V P, Schlagel D L and Lograsso T A 2004 *Phys. Rev. Lett.* **93** 237203
[38] Kittel C 1968 *Solid State Phys.* **22** 1
[39] Pecharsky V K, Samolyuk G D, Antropov V P, Pecharsky A O and Gschneidner K A Jr 2003 *J. Solid State Chem.* **171** 57
[40] Hernando A, Rojo J M, Gomez Sal J C and Novo J M 1996 *J. Appl. Phys.* **79** 4815
[41] Campbell I A 1972 *J. Phys. F: Met. Phys.* **2** L47
[42] Szade J and Skorek G 1999 *J. Magn. Magn. Mater.* **196/197** 699
[43] Zangrando M, Finazzi M, Paolucci G, Comelli G, Diviacco B, Walker R P, Cocco D and Parmigiani F 2001 *Rev. Sci. Instrum.* **72** 1313
[44] Zangrando M, Zacchigna M, Finazzi M, Cocco D, Rochow R and Parmigiani F 2004 *Rev. Sci. Instrum.* **75** 31
[45] Schlagel D L, Lograsso T A, Pecharsky A O and Sampaio J 2005 *Light Metals 2005* ed H Kvande (Warrendale, PA: The Minerals, Metals and Materials Society, TMS) p 1181
[46] Powell C J and Jablonski A 2000 *NIST Electron Inelastic-Mean-Free-Path Database*-Version 1.1 (Gaithersburg, MD: National Institute of Standards and Technology)
[47] Tanuma S, Powell C J and Penn D R 1994 *Surf. Interface Anal.* **17** 911
[48] Szade J and Neumann M 2001 *J. Phys.: Condens. Matter* **13** 2717
[49] Szade J, Lachnitt J and Neumann M 1997 *Phys. Rev.* B **55** 1430
[50] Gerken F, Barth J and Knuz C 1981 *Phys. Rev. Lett.* **47** 993
[51] López M F and Gutiérrez A 1997 *J. Phys.: Condens. Matter* **9** 6113
[52] Thole B T, Wang X D, Harmon B N, Li D Q and Dowben P A 1993 *Phys. Rev.* B **47** 9098
[53] Samolyuk G D and Antropov V P 2002 *J. Appl. Phys.* **91** 8541
[54] Schüssler-Langeheine C, Meier R, Ott H, Hu Z, Mazumdar C, Grigoriev A Y, Kaindl G and Weschke E 1999 *Phys. Rev.* B **60** 3449
[55] Gerken F 1983 *J. Phys. F: Met. Phys.* **13** 703